

Article

A Fuzzy Backstepping Attitude Control Based on an Extended State Observer for a Tilt-Rotor UAV

Suiyuan Shen ¹, Jinfa Xu ^{1,*} and Qingyuan Xia ²

¹ National Key Laboratory of Rotorcraft Aeromechanics, Nanjing University of Aeronautics & Astronautics, Nanjing 210016, China

² School of Computer Science and Engineering, Nanjing University of Science and Technology, Nanjing 210094, China

* Correspondence: xjfnuaa@163.com

Abstract: In order to overcome the influence of internal and external disturbances caused by rotor tilt motion and gust disturbance on the full flight mode control of a tilt-rotor unmanned aerial vehicle (UAV), a design method using fuzzy backstepping control based on an extended-state observer (FBS-ESO) is proposed. In this paper, fuzzy control is used to tune the parameters of the backstepping control law online, and the extended-state observer estimates the total disturbance of the controlled system to improve the controller's robustness and anti-disturbance capability. This paper designs the attitude control system of a tilt-rotor UAV based on an FBS-ESO controller. The control performance of the FBS-ESO controller is tested in a hardware-in-loop simulation of the attitude control system. The simulation results show that changing the rotor tilt angle will destroy the stability of the traditional backstepping controller and active disturbance rejection controller (ADRC). In contrast, the FBS-ESO controller maintains good control performance. In addition, the performance of the FBS-ESO controller is not significantly affected by adding external gust disturbance or changing the UAV parameters in the simulation. These disturbances significantly impact the traditional backstepping controller and ADRC. Therefore, the FBS-ESO controller has better anti-disturbance capabilities and robustness, as well as higher attitude control accuracy.

Keywords: tilt-rotor; unmanned aerial vehicle; extended-state observer; backstepping control; fuzzy control; attitude control; hardware-in-loop simulation



Citation: Shen, S.; Xu, J.; Xia, Q. A Fuzzy Backstepping Attitude Control Based on an Extended State Observer for a Tilt-Rotor UAV. *Aerospace* **2022**, *9*, 724. <https://doi.org/10.3390/aerospace9110724>

Received: 17 October 2022

Accepted: 15 November 2022

Published: 17 November 2022

Publisher's Note: MDPI stays neutral with regard to jurisdictional claims in published maps and institutional affiliations.



Copyright: © 2022 by the authors. Licensee MDPI, Basel, Switzerland. This article is an open access article distributed under the terms and conditions of the Creative Commons Attribution (CC BY) license (<https://creativecommons.org/licenses/by/4.0/>).

1. Introduction

An unmanned aerial vehicle (UAV) has many advantages: low cost, low loss, zero casualties, reusability, and high mobility [1–3]. Therefore, UAVs are widely used in military, civil, and scientific research. Compared with a fixed-wing UAV, a tilt-rotor UAV has unique vertical takeoff and landing characteristics, hovering capabilities, and maneuverability during flight, and so tilt-rotor UAVs have broader application prospects [4,5]. A tilt-rotor UAV has three flight modes: fixed-wing, transition flight, and helicopter. The aerodynamic characteristics of each mode are very different, and the nonlinearity and coupling are severe. Especially in the transition mode, with the tilt movement of the rotor, a UAV is in a variant process, and the structure and aerodynamics change significantly. Moreover, the coupling between the helicopter and the fixed-wing manipulation mechanisms is complex. The use of a traditional flight control system is challenging for realizing the stable control of the full flight mode of a tilt-rotor UAV [6–8]. Therefore, the realization of the full flight mode control of a tilt-rotor UAV is one of the research priorities in the academic community.

Researchers have proposed many flight control design methods for tilt-rotor UAVs. For example, using linear control, Papachristos et al. [9] designed a proportional integral derivative (PID) controller based on a transfer function for the pitch, roll, and yaw control loops. They analyzed the control performance using the root locus method and Bode diagram. The effectiveness of the PID controller was tested with a hovering experiment

on an actual flight platform. Houari et al. [10] verified that a linear quadratic regulator (LQR) is more robust than a PID controller in vertical takeoff and longitudinal motions, with an overshoot response time performance index and control accuracy as standards. The design of the linear control method was simple, but its performance was poor in the face of complex systems with nonlinear coupling and disturbance uncertainty. Moreover, the parameter tuning accuracy of the linear controller was low, and it was not suitable for a transition mode with serious disturbance and coupling. Therefore, the linear controller cannot effectively realize the full flight mode control of a tilt-rotor UAV. Compared with linear control, a nonlinear controller is effective in a wide range of flight envelopes and is conducive to giving full play to the advantages of the high maneuverability and high sensitivity of tilt-rotor UAVs. Cardoso et al. [11] designed an adaptive hybrid framework and selected a weight function to adjust an H_2/H_∞ hybrid controller to ensure a smooth transition between full flight modes. However, this controller was very complex, which is not conducive to engineering applications. Guo [12] divided a tilt-rotor UAV into several subsystems, established a model and controller for each subsystem, and ensured a smooth transition between controllers through a model adaptive control strategy. However, this method needed to design multiple controllers to increase the difficulty of control system design and depended on an accurate mathematical model, which is not conducive to engineering applications. Papachristos et al. [13–15] applied a model predictive control (MPC) to investigate a hovering experiment of a micro tilt-rotor UAV and provided the experimental results. The control loop was designed as a double-loop structure, and the inner loop was a PD-dD controller used for the attitude control of the UAV. By comparing the cost function values of different rotor tilt angles, the sub-model of the minimum value of the cost function was used as the outer loop MPC position controller. The above references used an MPC to improve the disturbance suppression in hovering states without paying attention to the transition or fixed-wing aircraft modes. At the same time, the prediction model of the MPC was not easy to establish, which increased the difficulty of the controller design. Liu [16] designed an exponential nonsingular terminal sliding mode surface, which could estimate and compensate for complex unknown disturbances online and improve the robustness of attitude control. However, the sliding mode controller switched back and forth near the sliding mode surface, resulting in a high-frequency chattering of the system, which seriously threatened the flight safety of the UAV. Balas and Casavola et al. [17–19] used LPV/qLPV controllers to solve the control problems of many complex strong coupling systems. The LPV/qLPV controller could fully consider the flight performance of the UAV, which is conducive to the realization of optimal control. Moreover, the above nonlinear controller was generally based on an accurate model and suppressed the system's internal and external uncertain disturbance by an indirect method. The control effect was significantly reduced when there was a strong disturbance or mechanical fault within the allowable range [20].

Therefore, researchers have tried to combine a nonlinear controller with other control methods to improve control performance. Some researchers have introduced intelligent control methods into nonlinear control, such as Autenrieb et al. [21], who applied a neural network to estimate the uncertain disturbance to improve a controller's performance. Hong et al. [22] constructed a fuzzy sliding mode controller for a UAV. They verified through simulation experiments that the stability of the fuzzy sliding mode control system was better than the pure sliding mode control system in the case of external disturbance. The intelligent control method could effectively improve the anti-disturbance and robustness of a nonlinear controller.

Active disturbance rejection control (ADRC) can effectively overcome the influence of internal and external disturbances [23–25]. The core of ADRC is to treat the internal and external disturbances of the system as the total disturbance, estimate the total disturbance through an extended-state observer (ESO), and use the ESO for real-time system compensation. An ESO can effectively track the total disturbance of a system in real-time, with strong adaptability and a simple structure. Wang et al. [26,27] designed a full mode flight

control system for a tilt-rotor UAV. The simulation and flight tests showed that the ADRC could effectively estimate and overcome the influence of the total disturbance of a tilt-rotor UAV. However, the state error nonlinear control law (SENCL) in the ADRC controller had a weak dynamic performance and poor rapidity [28]. The backstepping control had better dynamics and rapidity, which could compensate for the defects of SENCL [29,30]. Therefore, this paper absorbs the idea of an ESO in ADRC and proposes a fuzzy backstepping control based on an ESO (FBS-ESO). The disturbance of the external environment and the aerodynamic coupling between the rotor/wing and other components can be classified as external disturbance, according to the disturbance characteristics. The changes in its structural parameters caused by rotor tilt motion can be classified as an internal disturbance. The backstepping method designs a control law compensating for the internal and external total disturbances. An ESO is used to estimate the unknown total disturbances to realize the compensation of the control law. Fuzzy control can adaptively adjust the parameters of the backstepping control law online to improve the robustness of the controller. The FBS-ESO controller has the advantages of a simple design, easy implementation, and excellent control performance. An FBS-ESO controller can effectively overcome the influences of internal and external disturbances and meet the attitude control requirements of a tilt-rotor UAV in full flight mode.

The rest of this paper is arranged as follows: the second section describes the design of the FBS-ESO controller of the second-order nonlinear system. The third section describes the design of the attitude control system based on the FBS-ESO controller. In the fourth section, the attitude control hardware-in-loop simulation of the tilt-rotor UAV is described to prove the effectiveness of the FBS-ESO control method proposed in this paper. Finally, the fifth section draws the conclusions for this paper.

2. Design of the FBS-ESO Controller for the Second-Order System

2.1. Second-Order Nonlinear Expansion System

The second-order nonlinear uncertain plant including internal and external disturbances is as follows:

$$\begin{cases} \dot{x}_1 = x_2 \\ \dot{x}_2 = f(x, w, t) + b(t)u \\ y = x_1 \end{cases}, \quad (1)$$

where u and y are the input and output signals, $f(x, w, t)$ is a nonlinear function with an unknown disturbance, and $b(t)$ is an unknown function.

If we let $x_3 = f(x, w, t) + (b(t) - b_0)u$ represent the new expanded-state variable, x_3 contains an internal disturbance and an external disturbance, b_0 is a constant, and $\dot{x}_3 = g(t)$, then system (1) becomes an extended system with three state variables, as follows:

$$\begin{cases} \dot{x}_1 = x_2 \\ \dot{x}_2 = x_3 + b_0u \\ \dot{x}_3 = g(t) \\ y = x_1 \end{cases}. \quad (2)$$

2.2. Fuzzy Backstepping Control Law

The errors between the output of system (2) and the target state (command signal x_g) are:

$$e_1 = x_1 - x_g \quad (3)$$

$$\dot{e}_1 = \dot{x}_1 - \dot{x}_g = x_2 - \dot{x}_g \quad (4)$$

(1) Define the Lyapunov function $V = \frac{e_1^2}{2}$, then

$$\dot{V}_1 = e_1 \dot{e}_1 = e_1(x_2 - \dot{x}_g), \quad (5)$$

and if we can take the virtual control quantity $e_2 = x_2 + c_1 e_1 - \dot{x}_g$, then $\dot{V}_1 = -c_1 e_1^2 + e_1 e_2$ when $c_1 > 0, e_2 = 0, \dot{V}_1 \leq 0$. Therefore, it is necessary to design the control law to make $e_2 = 0$.

- (2) Define the Lyapunov function $V_2 = V_1 + \frac{e_2^2}{2}$ and differential the virtual control quantity:

$$\dot{e}_2 = x_3 + b_0 u + c_1 \dot{e}_1 - \ddot{x}_g. \quad (6)$$

Then,

$$\dot{V}_2 = \dot{V}_1 + e_2 \dot{e}_2 = -c_1 e_1^2 + e_1 e_2 + e_2 (x_3 + b_0 u + c_1 \dot{e}_1 - \ddot{x}_g). \quad (7)$$

To make the system meet the Lyapunov stable, it is required that $\dot{V}_2 \leq 0$, and the design control law is:

$$u = \frac{1}{b_0} (-x_3 - c_1 \dot{e}_1 + \ddot{x}_g - c_2 e_2 - e_1). \quad (8)$$

Then,

$$\dot{V}_2 = -c_1 e_1^2 - c_2 e_2^2 \quad (9)$$

when $c_1 = c_2 = \frac{\eta}{2}, c_2 > 0$, and

$$\dot{V}_2 = -\eta V_2. \quad (10)$$

If we integrate $\frac{1}{V_2} dV_2 = -\eta dt$ to get

$$\int_0^t \frac{1}{V_2} dV_2 = \int_0^t -\eta dt, \quad (11)$$

then

$$V_2(t) = V_2(0) e^{-\eta t}. \quad (12)$$

The formula $V_2(t) = \frac{e_1^2}{2} + \frac{e_2^2}{2}$, $V_2(t)$ converges exponentially, and so when $t \rightarrow \infty$, $e_1 \rightarrow 0, e_2 \rightarrow 0$, and when $e_2 = x_2 + c_1 e_1 - \dot{x}_g$, then $x_2 \rightarrow \dot{x}_g$. Thus, it is ensured that the system state quantities x_1 and x_2 can quickly track the command signals x_g and \dot{x}_g .

In the formula $c_1 = c_2 = \frac{\eta}{2}$, for the backstepping control law (8), two parameters η and b_0 need to be adjusted, and η and b_0 affect the dynamics and stability of the control system, respectively. At the same time, with the change in the flight state and the external environment of the tilt-rotor UAV, the fixed η and b_0 cannot meet the control requirements, resulting in a decline in control performance. Therefore, according to the variation in error e_1 and e_2 , this paper adopts fuzzy control to adjust η and b_0 online automatically so that the controller can adapt to the variations in flight environment and disturbance. The operation process of the fuzzy control is shown in Figure 1. The input of the controller is e_1 and e_2 and the output is the adjustment $\Delta\eta$ and Δb_0 of η and b_0 . Firstly, $e_1, e_2, \Delta\eta$, and Δb_0 are fuzzification, and then the fuzzy parameters of $\Delta\eta$ and Δb_0 are obtained by fuzzy reasoning, according to fuzzy rules. Finally, the actual values of $\Delta\eta$ and Δb_0 are obtained by ambiguity resolution.

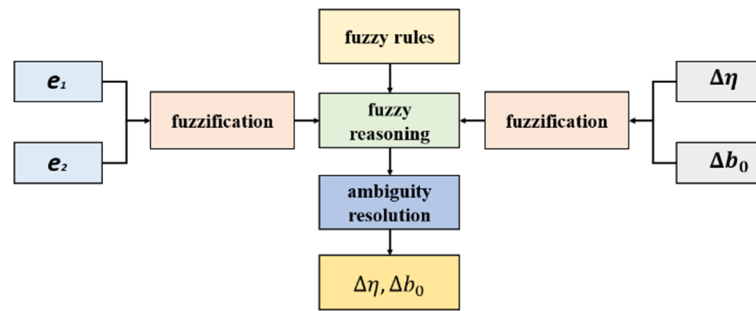


Figure 1. The η and b_0 correction algorithm based on fuzzy control.

The η and b_0 of the backstepping control law are:

$$\begin{cases} \eta(t + 1) = \eta(t) + \Delta\eta(t) \\ b_0(t + 1) = b_0(t) + \Delta b_0(t) \end{cases} \quad (13)$$

(1) Fuzzy Rules

The input and output variables of the fuzzy controller are defined as five fuzzy levels in their respective domains: negative big (NB), negative small (NS), zero (ZO), positive small (PS), and positive big (PB). The membership function is triangular, as shown in Figure 2.

(2) Fuzzy Reasoning

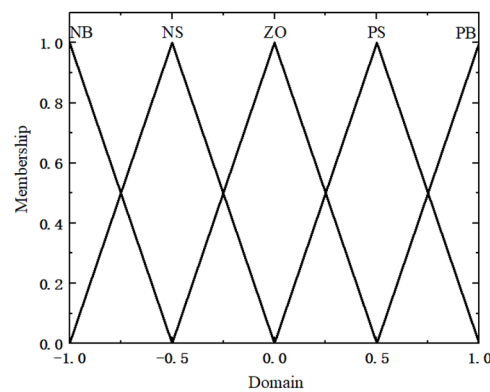


Figure 2. Triangular membership function.

According to the parameter tuning method of the backstepping controller, the fuzzy rules of $\Delta\eta$ and Δb_0 are formulated as shown in Tables 1 and 2.

(3) Ambiguity Resolution

Table 1. Fuzzy rules of $\Delta\eta$.

		e_2				
		NB	NS	ZO	PS	PB
e_1	NB	PB	PS	PS	PS	ZO
	NS	PB	PS	PS	ZO	ZO
	ZO	PS	PS	ZO	ZO	NS
	PS	PS	ZO	NS	NS	NS
	PB	ZO	ZO	NS	NS	NB

Table 2. Fuzzy rules of Δb_0 .

Δb_0		e_2				
		NB	NS	ZO	PS	PB
e_1	NB	NB	NB	NS	NS	PS
	NS	NS	NS	ZO	ZO	PS
	ZO	NS	ZO	PS	PS	PS
	PS	NS	ZO	ZO	PS	PB
	PB	ZO	PS	PS	PB	PB

The membership of $\Delta\eta$ and Δb_0 under the current input value can be obtained using fuzzy rules. The center of gravity method is used to calculate $\Delta\eta$ and Δb_0 in the domain, that is:

$$\Delta\eta, \Delta b_0 = \frac{\sum_{i=1}^N g_i S_i}{\sum_{i=1}^N S_i} \tag{14}$$

where S_i, g_i , and N are the membership, fuzzy quantitative value, and fuzzy level, respectively.

2.3. Extended State Observer

The control law (8) needs to solve the unknown total disturbance x_3 . The effective solution is to design an extended-state observer to obtain the control law variables by estimating the state variables and the extended total disturbance.

The extended-state observer of the second-order system (2) is [20]:

$$\begin{cases} e = \hat{x}_1 - y \\ \dot{\hat{x}}_1 = \hat{x}_2 - \beta_1 e \\ \dot{\hat{x}}_2 = \hat{x}_3 - \beta_2 fal(e, \lambda_1, \zeta) + b_0 u \\ \dot{\hat{x}}_3 = -\beta_3 fal(e, \lambda_2, \zeta) \end{cases} \tag{15}$$

$$fal(e, \lambda, \zeta) = \begin{cases} \frac{e}{\zeta^{1-\lambda}}, & |e| \leq \zeta, \\ |e|^\lambda sign(e), & |e| > \zeta, \end{cases} \tag{16}$$

where $\lambda_i (i = 1, 2)$ and $\beta_i (i = 1, 2, 3)$ are the gain coefficients, ζ is the step size, and $fal(e, \lambda, \zeta)$ is a nonlinear function. The three state variables of the extended state observer (15) can track the state variables and total disturbances of the system (2) [20] as follows:

$$\hat{x}_1 \rightarrow x_1, \hat{x}_2 \rightarrow x_2, \hat{x}_3 \rightarrow x_3. \tag{17}$$

The backstepping control law of equation (8) is rewritten as:

$$\begin{cases} u = \frac{1}{b_0} (-\hat{x}_3 - c_1 \dot{e}_1 + \ddot{x}_g - c_2 e_2 - \dot{e}_1) \\ e_1 = \hat{x}_1 - x_g \\ e_2 = \hat{x}_2 + c_1 e_1 - \dot{x}_g \end{cases} . \tag{18}$$

In summary, the block diagram of the FBS-ESO controller is as shown in Figure 3.

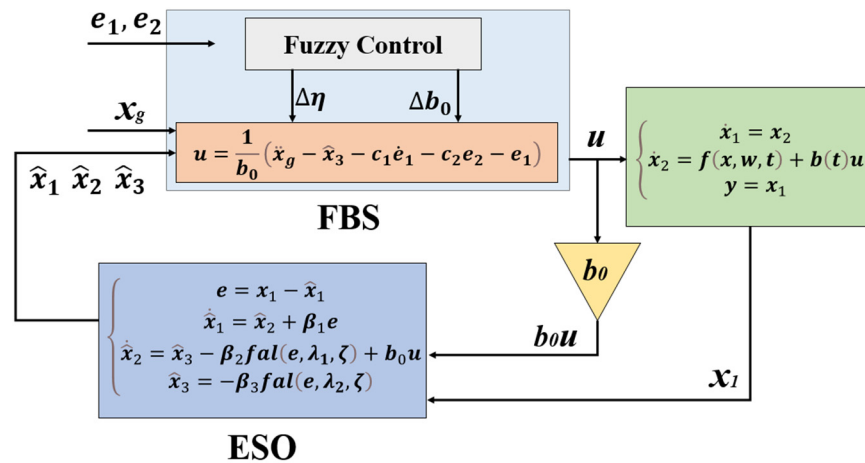


Figure 3. Block diagram of the FBS-ESO controller.

3. Attitude Control Design of the Tilt-Rotor UAV

The attitude control system of the tilt-rotor UAV is shown in Figure 4, including the FBS-ESO attitude controller, manipulation strategy, and flight dynamics model. The FBS-ESO attitude controller calculates the control quantities of the three loops of roll, pitch, and yaw according to the input and output information of the system, and then it assigns the control quantities to each control surface of the tilt-rotor UAV through the manipulation strategy to act on the flight dynamics model of the tilt-rotor UAV. Under the action of aerodynamics, the attitude of the tilt-rotor UAV changes.

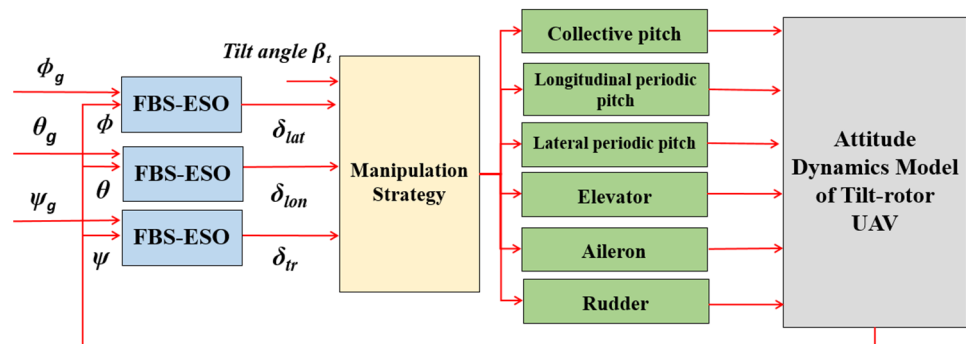


Figure 4. Attitude control system of the tilt-rotor UAV.

3.1. Attitude Dynamics Model

According to reference [31], the attitude nonlinear dynamic model of a tilt-rotor UAV is:

$$\begin{bmatrix} \dot{\phi} \\ \dot{\theta} \\ \dot{\psi} \\ \dot{p} \\ \dot{q} \\ \dot{r} \end{bmatrix} = \begin{bmatrix} p + d_\phi \\ q + d_\theta \\ r + d_\psi \\ (c_1 r + c_2 p)q + c_3 L + c_4 N \\ c_5 p r - c_6 (p^2 - r^2) + c_7 M \\ (c_8 p - c_2 r)q + c_4 L + c_9 N \end{bmatrix}, \quad (19)$$

where:

$$\begin{cases} d_\phi = (r \cos \phi + q \sin \phi) \tan \theta \\ d_\theta = (\cos \phi - 1)q - r \sin \phi \\ d_\psi = \left(\frac{\cos \phi}{\cos \theta} - 1\right)r + q \frac{\sin \phi}{\cos \theta} \\ L = Qc_{lat}C_l^{lat}\delta_{lat} \\ M = Qc_{lon}C_l^{lon}\delta_{lon} \\ N = Qc_{tr}C_l^{tr}\delta_{tr} \\ Q = 0.5\rho V^2 \end{cases} \quad \text{and} \quad (20)$$

$$\begin{cases} c_1 = \frac{(I_x - I_z)I_z - I_{xz}}{C_0}, c_2 = \frac{(I_x - I_y + I_z)I_{xz}}{C_0} \\ c_2 = \frac{I_z}{C_0}, c_4 = \frac{I_{xz}}{C_0}, c_5 = \frac{I_z - I_x}{I_y}, c_6 = \frac{I_{xz}}{I_y} \\ c_7 = \frac{1}{I_y}, c_8 = \frac{(I_x - I_y)I_x - I_{xz}^2}{C_0}, c_9 = \frac{I_x}{C_0} \end{cases} \quad (21)$$

where ϕ , θ , and ψ are the Euler angles of roll, pitch, and yaw, respectively; p , q , and r are the angular velocities; L , M , and N are the moments of the components of the whole vehicle (rotor, fuselage, vertical tail, flat tail, wing, etc., including gravity); I_x , I_y , I_z , and I_{xz} are the inertia; $C_0 = I_x I_z - I_{xz}^2$, c_{lat} , c_{lon} , and c_{tr} are the distances between the force and the center of gravity; C_l^{lat} , C_l^{lon} , and C_l^{tr} are the moment coefficients; δ_{lat} , δ_{lon} , and δ_{tr} are the control amounts of roll angle, pitch angle, and yaw angle, respectively; ρ is the air density; and V is the relative incoming velocity.

3.2. Attitude Control Law

If we define the following variables:

$$\begin{cases} \mathbf{x}_1 = [\phi \ \theta \ \psi]^T, \mathbf{x}_2 = [p \ q \ r]^T \\ \mathbf{u} = [\delta_{lat} \ \delta_{lon} \ \delta_{tr}]^T \\ \mathbf{d}_1 = [d_\phi \ d_\theta \ d_\psi]^T, \mathbf{d}_2 = [c_4 N \ 0 \ c_9 N]^T \\ f(\mathbf{x}_2) = [(c_1 r + c_2 p)q \ c_5 p r - c_6(p^2 - r^2) \ (c_8 p - c_2 r)q]^T \\ \mathbf{b} = [Qc_3 c_{lat} C_l^{lat} \ Qc_7 c_{lon} C_l^{lon} \ Qc_9 c_{tr} C_l^{tr}]^T \end{cases} \quad (22)$$

then we can obtain the following by combining Equations (19) and (20):

$$\begin{cases} \dot{\mathbf{x}}_1 = \mathbf{x}_2 + \mathbf{d}_1 \\ \dot{\mathbf{x}}_2 = f(\mathbf{x}_2) + \mathbf{b}\mathbf{u} + \mathbf{d}_2 \end{cases} \quad (23)$$

From Equation (23), we can obtain:

$$\ddot{\mathbf{x}}_1 = \dot{\mathbf{x}}_2 + \dot{\mathbf{d}}_1 = f(\mathbf{x}_2) + \mathbf{b}\mathbf{u} + \mathbf{d}_2 + \dot{\mathbf{d}}_1 = f(\mathbf{x}_2) + \mathbf{d}_2 + \dot{\mathbf{d}}_1 + (\mathbf{b} - \mathbf{b}_0)\mathbf{u} + \mathbf{b}_0\mathbf{u}, \quad (24)$$

where \mathbf{b}_0 is the attitude control gain matrix and the expanded state quantity \mathbf{x}_3 is defined as:

$$\begin{cases} \mathbf{x}_3 = f(\mathbf{x}_2) + \mathbf{d}_2 + \dot{\mathbf{d}}_1 + (\mathbf{b} - \mathbf{b}_0)\mathbf{u} \\ \mathbf{g}(t) = \dot{\mathbf{x}}_3 \end{cases} \quad (25)$$

Then, Equation (24) is transformed into a second-order nonlinear expansion system (26) in the form of Equation (2):

$$\begin{cases} \dot{\mathbf{x}}_1 = \mathbf{x}_2 \\ \dot{\mathbf{x}}_2 = \mathbf{x}_3 + \mathbf{b}_0\mathbf{u} \\ \dot{\mathbf{x}}_3 = \mathbf{g}(t) \end{cases} \quad (26)$$

Therefore, the pitch, roll, and yaw attitude control loops can all be designed as a second-order FBS-ESO control structure. The attitude control loop's output is superimposed with the trim base offset to form the $[\delta_{lon} \ \delta_{lat} \ \delta_{tr}]$ acts on the tilt-rotor UAV.

From the foregoing analysis, the longitudinal pitch control δ_{lon} is designed as:

$$\begin{cases} e = \hat{x}_1 - \theta, \dot{\hat{x}}_1 = \hat{x}_2 - \beta_1 e \\ \dot{\hat{x}}_2 = \hat{x}_3 - \beta_2 fal(e, \lambda_1, \zeta) + b_{0\theta} u \\ \dot{\hat{x}}_3 = -\beta_3 fal(e, \lambda_2, \zeta) \\ e_1 = \hat{x}_1 - \theta_g, e_2 = \hat{x}_2 + c_1 e_1 - \dot{\theta}_g \\ u = \frac{1}{b_{0\theta}} \left(-\hat{x}_3 - 0.5\eta_\theta \dot{e}_1 + \ddot{\theta}_g - 0.5\eta_\theta e_2 - e_1 \right) \\ b_{0\theta}(t+1) = b_{0\theta}(t) + \Delta b_{0\theta}(t), \eta_\theta(t+1) = \eta_\theta(t) + \Delta \eta_\theta(t) \\ \delta_{lon} = u + \delta_\theta^{trim} \end{cases}, \tag{27}$$

where θ_g is the target pitch attitude angle command signal, θ is the actual pitch angle of the tilt-rotor UAV, δ_θ^{trim} is the longitudinal control trim, $b_{0\theta}$ and η_θ are the attitude control gains, $\Delta b_{0\theta}$ and $\Delta \eta_\theta$ are the adjustments of $b_{0\theta}$ and η_θ for the output of the fuzzy control, \hat{x}_1 and \hat{x}_2 are the estimated values of the angle and differential value, and \hat{x}_3 is the estimate of the total disturbance.

The design of the roll loop control δ_{lat} and the yaw loop control δ_{tr} are similar and will not be repeated.

3.3. Manipulation Strategy

The manipulation strategy of the tilt-rotor UAV is shown in Table 3. The control weight coefficient is used to adjust the control influence degree of each control surface in different flight modes to ensure the smooth transition of the UAV. The control weight coefficient adopts trigonometric function:

$$\begin{cases} \omega_r = \sin \beta_t \\ \omega_q = \cos \beta_t \end{cases}, \tag{28}$$

where ω_r is the control weight coefficient of the rotor, ω_q is the control weight coefficient of the fixed wing's control surface, and β_t is the tilt angle. When $\beta_t = 90^\circ$ is the helicopter mode, when $\beta_t = 0^\circ$ is the fixed wing mode, and when the tilt-rotor UAV transitions from helicopter mode to fixed wing mode, the control weight coefficient of the rotor gradually decreases from 1 to 0 while the control weight coefficient of the fixed-wing aircraft gradually increases from 0 to 1 to complete the smooth transition of the tilt-rotor UAV. The manipulation quantity is as shown in Equation (29):

$$\begin{cases} \delta_{zxx} = \delta_{lon}\omega_r - \delta_{tr}\omega_r \\ \delta_{zxy} = \delta_{lon}\omega_r + \delta_{tr}\omega_r \\ \delta_{zjz} = \delta_{col} - \delta_{lat}\omega_r \\ \delta_{zjy} = \delta_{col} + \delta_{lat}\omega_r, \delta_{fxd} = \delta_{tr}\omega_q \\ \delta_{fy} = \delta_{lat}\omega_q, \delta_{sjd} = \delta_{lon}\omega_q \end{cases}, \tag{29}$$

where δ_{zxx} and δ_{zjz} are the longitudinal periodic variation and collective of the left rotor, respectively; δ_{zxy} and δ_{zjy} are the longitudinal periodic variation and collective of the right rotor, respectively; δ_{fxd} , δ_{fy} , and δ_{sjd} are the control quantity of rudder, aileron, and elevator, respectively; and δ_{col} is the collective pitch reference of the rotor.

Table 3. Control strategy of the tilt-rotor UAV.

Mode	Roll	Pitch	Yaw
helicopter mode	collective differential	longitudinal variation	longitudinal variation differential
transition mode	collective differential plus aileron	longitudinal variation plus elevator	longitudinal variation differential plus rudder
fixed-wing mode	aileron	elevator	rudder

4. Attitude Control Verification of the Tilt-Rotor UAV

4.1. Hardware-in-Loop Simulation System

Hardware-in-loop (HIL) systems provide a virtual flight environment and a mathematical model of a UAV, but they use the key hardware of flight control systems. HIL simulation has high credibility. HIL is more reliable than pure digital simulation [32]. Compared with physical simulation, HIL simulation has lower costs and higher efficiency. As shown in Figure 5, the real-time HIL simulation system of the unmanned helicopter built in this paper adopts the flight control computer with STM32F405ZGT6 as the core processor. In the Keil environment, the FBS-ESO attitude control law is written as C code to run in the flight control computer. The attitude dynamics model of the tilt-rotor UAV is built based on MATLAB/SIMULINK numerical simulation software. The operation process of the HIL simulation system is as follows: the ground control station transmits the target attitude command to the flight control computer via the radio station. The flight control computer runs the FBS-ESO attitude control law and calculates the manipulation amount of the rotor and rudder surfaces, according to the target and actual attitude. Then, the manipulation amount is transmitted to MATLAB/SIMULINK through serial communication. We use the Serial Receive module in SIMULINK to receive the data of the manipulation amount. After the data is unpacked, it acts on the attitude dynamics model of the tilt-rotor UAV to obtain the real-time attitude. Finally, the actual attitude is transmitted to the FlightGear visual simulation software and flight control computer through the Serial Send module. FlightGear can display the three-dimensional flight animation of the tilt-rotor UAV in real-time, and the flight control computer stores the actual attitude and target attitude in the SD data memory card, which is convenient for subsequent data analysis.

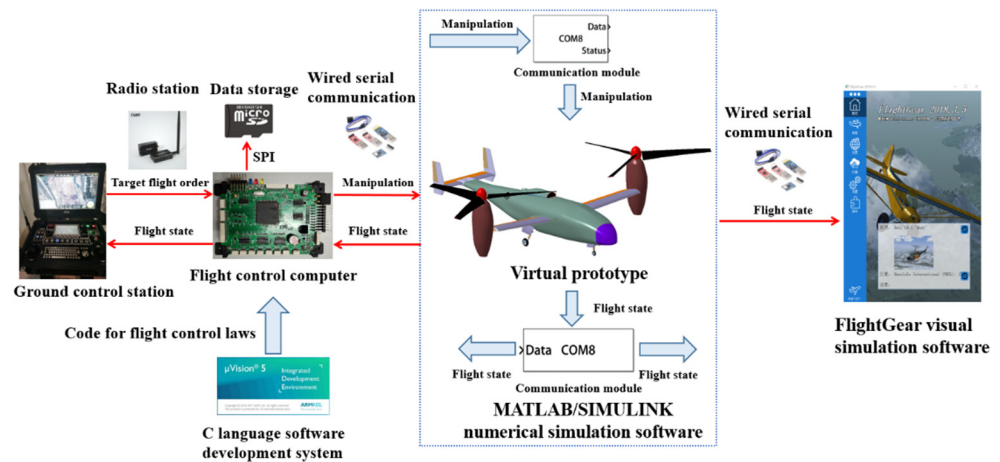


Figure 5. Composition diagram of the HIL simulation system of the tilt-rotor UAV.

4.2. Attitude Control Test

The controlled plant in this paper is shown in the Figure 6. The tilt-rotor UAV changes the tilt angle of the rotor to realize the transition from helicopter mode to fixed-wing mode. The basic parameters of the tilt-rotor UAV are shown in the initial values in Table 4. The attitude controller adopts the BS, ADRC, and FBS-ESO controller designed in this paper. The initial parameters of the FBS-ESO controller and the parameters of the BS controller and ADRC controller are shown in Table 5. The above three controllers operate in the hardware-in-loop simulation system.

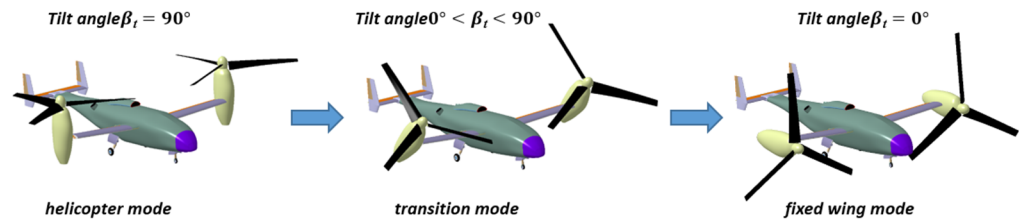


Figure 6. Schematic diagram of the tilt-rotor UAV.

Table 4. Parameters of the tilt-rotor UAV.

Parameter	Unit	Initial Value	Modify Value
total weight	kg	3000	2400
rotor radius	m		3
number of blades	-		3
rotor velocity	rad/s		70
wing area	m ²		10
I_x	kg·m ²	7391	5912
I_y	kg·m ²	48,847	39,000
I_z	kg·m ²	52,524	42,000

Table 5. Parameters of the controllers.

$[\phi \ \theta \ \psi]$	BS	ADRC	FBS-ESO
b_0	[4 1 1]	[10 2 5]	[4 1 1]
c_1	[160 150 120]	-	[160 150 120]
c_2	[160 150 120]	-	[160 150 120]
r	-	[10 10 10]	-
h	-	[0.5 0.5 0.5]	-
β_{01}	-	[20 56 12]	-
β_{02}	-	[2 7 3]	-
β_1	-	[1 4 12]	[4 24 50]
β_2	-	[10 24 28]	[65 80 80]
β_3	-	[10 12 10]	[5 8 2]
ζ	-	[0.01 0.01 0.01]	[0.01 0.01 0.01]
$\lambda_{1,2}$	-	[0.25 0.25 0.75]	[0.5 0.5 0.5]

4.2.1. Stability Test

The initial attitude angle of the tilt-rotor UAV is 0° , the expected target value is 10° , and the simulation time is 10 s. If we keep the parameters of the attitude controller in Table 5 unchanged and conduct the attitude control simulation experiments of 90° , 45° , and 0° of the rotor tilt angle, respectively, then the simulation results are as shown in Figure 7. The simulation results show that the FBS-ESO controller has the best control effect under the three flight modes. The rise time of the FBS-ESO controller is short, and the overshoot, steady-state error, and vibration amplitude are slight. The decreased rotor tilt angle decreases the ADRC and BS controller performance gradually. The ADRC controller has obvious chattering and overshoot when switching to fixed-wing mode. In contrast, the performance of the BS controller decreases more violently. It cannot control the pitch and yaw angle, indicating that the ADRC and BS controller cannot realize the full mode attitude control of a tilt-rotor UAV. The performance of the FBS-ESO controller does not change significantly with the change in tilt angle and has the attitude control ability of full flight mode.

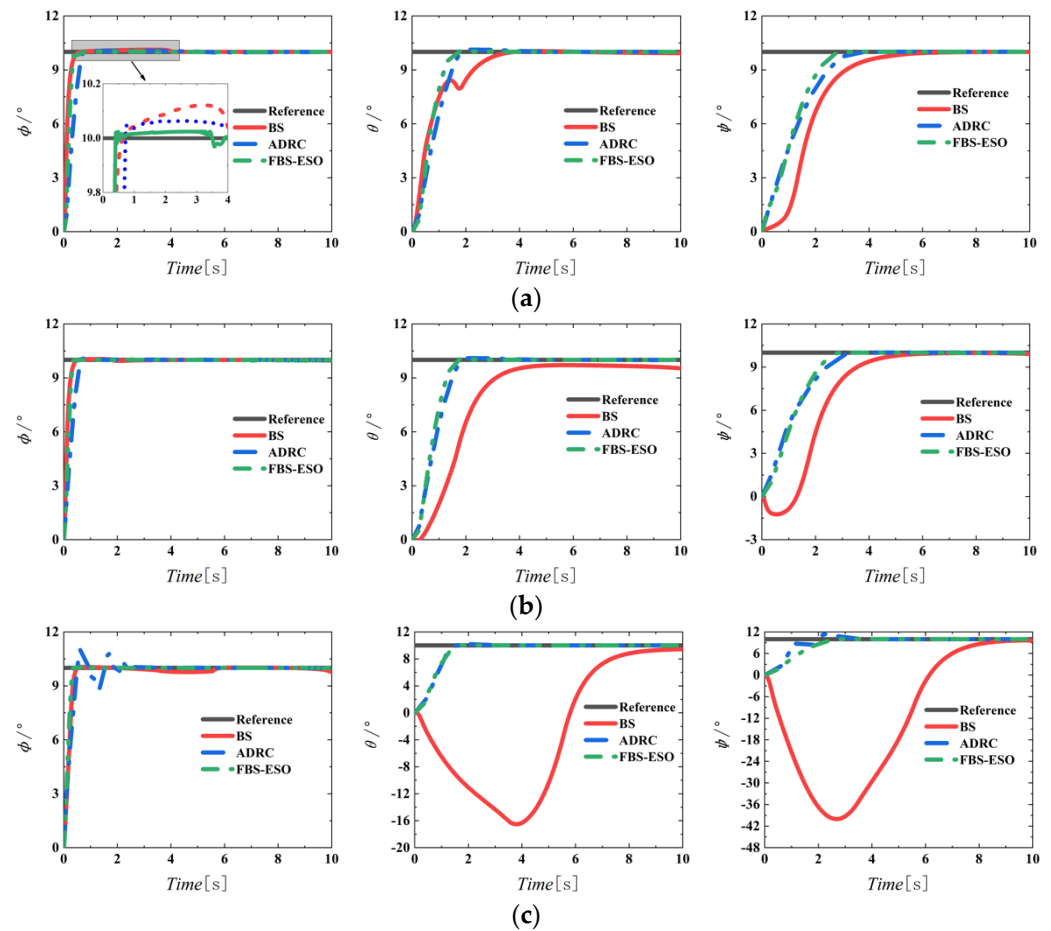


Figure 7. Response curves of the steady-state tests. (a) $\beta_t = 90^\circ$ (helicopter mode); (b) $\beta_t = 45^\circ$ (transition mode); and (c) $\beta_t = 0^\circ$ (fixed-wing mode).

4.2.2. Anti-Disturbance Test

The external wind disturbance will interfere with the flight of a tilt-rotor UAV. A rectangular wave signal simulates the sudden wind disturbance in a period. At the fifth second, a rectangular wave with an amplitude of 20 and pulse width of 3 s is added to the three-axis incoming velocity term of the nonlinear flight dynamics model as the external disturbance to test the anti-disturbance of the attitude controllers. If we keep the controller parameters in Table 5 unchanged, then the simulation results are as shown in Figure 8. When the external disturbance is added to the UAV, the FBS-ESO controller has good stability in any flight mode. The BS controller fluctuates the most, the roll angle has a noticeable rectangular jump, and the pitch angle and yaw angle fluctuate obviously. The results above show that the FBS-ESO controller has a better anti-disturbance ability.

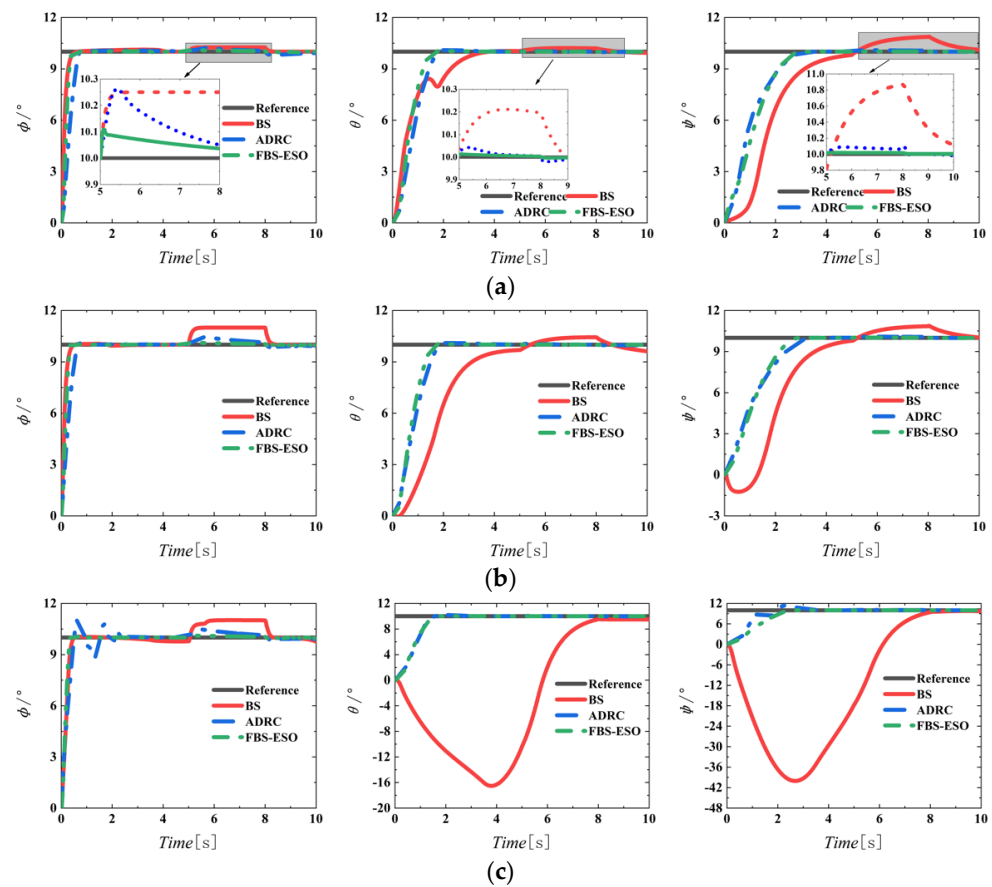


Figure 8. Response curves of the anti-disturbance tests. (a) $\beta_t = 90^\circ$ (helicopter mode); (b) $\beta_t = 45^\circ$ (transition mode); and (c) $\beta_t = 0^\circ$ (fixed-wing mode).

4.2.3. Robustness Test

We can change the parameter value of the tilt-rotor UAV as an internal disturbance to simulate the parameter uncertainty of the UAV. The modified values in Table 4 are controlled plants. The controller parameters in Table 5 are still used, the attitude control simulation of attitude controllers for the tilt-rotor UAV is carried out again, and the results are shown in Figure 9. The simulation results show that even if the dynamic characteristics of the controlled plant change significantly, the FBS-ESO controller can still achieve an excellent dynamic response curve under full flight mode, and the control performance is excellent. The ADRC and BS controller performance decrease significantly compared with the steady-state test. When the rotor tilts, the performance of the BS controller decreases rapidly, and the BS controller cannot effectively control the attitude angle of the tilt-rotor UAV, which shows that the FBS-ESO controller has strong robustness.

Based on the stability test, anti-disturbance test, and robustness test, it can be found that the FBS-ESO controller can better overcome the internal and external disturbances encountered by a tilt-rotor UAV in actual flight than a traditional backstepping controller and ADRC. The FBS-ESO controller is more suitable for the full flight mode control of the tilt-rotor UAV.

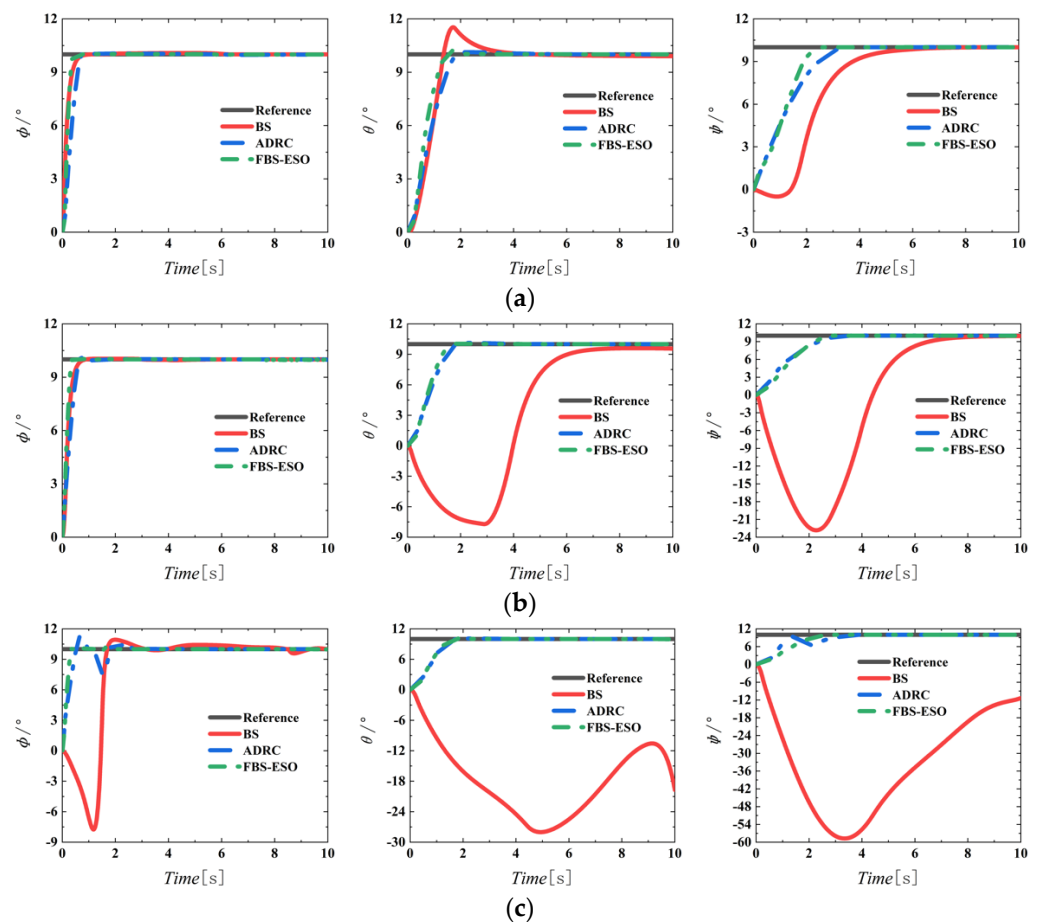


Figure 9. Response curves of the robustness tests. (a) $\beta_t = 90^\circ$ (helicopter mode); (b) $\beta_t = 45^\circ$ (transition mode); and (c) $\beta_t = 0^\circ$ (fixed-wing mode).

5. Conclusions

This paper proposes a design method for a fuzzy backstepping controller based on an extended-state observer. Fuzzy control is used to tune the parameters of the backstepping control law online, and the extended-state observer estimates the total disturbance of the controlled system. Through the hardware-in-loop simulation of attitude control of tilt-rotor UAV, the following conclusions are drawn in this paper:

- (1) Changing the rotor tilt angle will destroy the stability of a traditional backstepping controller and ADRC. In contrast, the FBS-ESO controller maintains good control performance.
- (2) The performance of the FBS-ESO controller will not be significantly affected by adding an external gust disturbance or changing the UAV parameters in the simulation. These disturbances significantly impact a traditional backstepping controller and ADRC.

Author Contributions: Conceptualization, S.S. and J.X.; methodology, S.S.; software, Q.X.; validation, S.S.; formal analysis, S.S.; investigation, S.S.; resources, J.X. and Q.X.; data curation, S.S.; writing—original draft preparation, J.X.; writing—review and editing, Q.X.; visualization, Q.X.; supervision, S.S.; project administration, J.X.; funding acquisition, S.S. All authors have read and agreed to the published version of the manuscript.

Funding: This paper is supported by the National Key Laboratory of Rotorcraft Aeromechanics Fund Program of China (61422202204 and 9140C400504130C4148) and the Priority Academic Program Development of Jiangsu Higher Education Institutions of China.

Institutional Review Board Statement: Not applicable.

Informed Consent Statement: Not applicable.

Data Availability Statement: Not applicable.

Conflicts of Interest: The authors declare no conflict of interest.

References

1. Halbe, O.; Hajek, M. A continuous multivariable finite-time super-twisting attitude and rate controller for improved rotorcraft handling. *Aerospace* **2022**, *9*, 6. [\[CrossRef\]](#)
2. Stojaković, P.; Rašuo, B. Single propeller airplane minimal flight speed based upon the lateral maneuver condition. *Aerosp. Sci. Technol.* **2016**, *49*, 239–249. [\[CrossRef\]](#)
3. Stojaković, P.; Velimirović, K.; Rašuo, B. Power optimization of a single propeller airplane take-off run on the basis of lateral maneuver limitations. *Aerosp. Sci. Technol.* **2018**, *72*, 553–563. [\[CrossRef\]](#)
4. Ducard, G.; Allenspach, M. Review of designs and flight control techniques of hybrid and convertible VTOL UAVs. *Aerosp. Sci. Technol.* **2021**, *8*, 1–25. [\[CrossRef\]](#)
5. Lu, K.; Tian, H.; Zhen, P.; Lu, S.; Chen, R. Conversion flight control for tiltrotor aircraft via active disturbance rejection control. *Aerospace* **2022**, *9*, 155. [\[CrossRef\]](#)
6. Rohr, D.; Studiger, M.; Stastny, T.; Lawrance, N.R.J.; Siegwart, R. Nonlinear model predictive velocity control of a VTOL tiltwing UAV. *IEEE Robot. Autom. Lett.* **2021**, *6*, 5776–5783. [\[CrossRef\]](#)
7. Toth, R. *Modeling and Identification of Linear Parameter-Varying Systems*; Springer: Berlin/Heidelberg, Germany, 2010.
8. Zheng, P.; Tan, X.; Kocer, B.B.; Yang, E.; Kovac, M. TiltDrone: A fully-actuated tilting quadrotor platform. *IEEE Robot. Autom. Lett.* **2022**, *5*, 6845–6852. [\[CrossRef\]](#)
9. Papachristos, C.; Alexis, K.; Tzes, A. Design and Experimental Attitude Control of an Unmanned Tilt-Rotor Aerial Vehicle. In Proceedings of the 15th International Conference on Advanced Robotics, Tallinn, Estonia, 20–23 June 2011; pp. 3297–3303.
10. Houari, A.; Bachir, I.; Mohamed, D.K. PID vs LQR controller for tilt-rotor airplane. *Int. J. Electr. Comput. Eng.* **2020**, *10*, 6309–6318. [\[CrossRef\]](#)
11. Cardoso, D.N.; Raffo, G.V.; Esteban, S. A Robust Adaptive Mixing Control for Improved Forward Flight of a Tilt-Rotor UAV. In Proceedings of the IEEE 19th International Conference on Intelligent Transportation Systems (ITSC), Windsor Oceanico Hotel, Rio de Janeiro, Brazil, 1–4 November 2016; pp. 273–281.
12. Guo, J.D.; Song, Y.G.; Xia, P.Q. Design for model fusion and robust controller of tilt-rotor aircraft. *J. Nanjing Univ. Aeronaut. Astronaut.* **2011**, *43*, 393–398.
13. Papachristos, C.; Alexis, K.; Tzes, A. Model Predictive Hovering-Translation Control of an Unmanned Tri-Tiltrotor. In Proceedings of the 2013 IEEE International Conference on Robotics and Automation, Karlsruhe, Germany, 6–10 May 2013; pp. 659–667.
14. Papachristos, C.; Alexis, K.; Tzes, A. Technical activities execution with a tiltrotor UAS employing explicit model predictive control. In Proceedings of the 19th World Congress the International Federation of Automatic Control, Cape Town, South Africa, 24–29 August 2014; pp. 156–162.
15. Papachristos, C.; Alexis, K.; Tzes, A. Dual-authority thrust-vectoring of a tri-tiltrotor employing model predictive control. *J. Intell. Robot. Syst.* **2015**, *81*, 1–34. [\[CrossRef\]](#)
16. Liu, H.; Wang, H.; Sun, J. Attitude control for QTR using exponential nonsingular terminal sliding mode control. *J. Syst. Eng. Electron.* **2019**, *30*, 191–200.
17. Casavola, G.; Gagliardi, A. Fault Detection and Isolation of Electrical Induction Motors via LPV Fault Observers. *IFAC Proc. Vol.* **2012**, *45*, 800–805. [\[CrossRef\]](#)
18. Marcos, A.; Balas, G.J. Development of linear parameter varying models for aircraft. *J. Guid. Control Dyn.* **2004**, *27*, 218–228. [\[CrossRef\]](#)
19. Shin, J.Y.; Balas, G.; Kaya, A. Blending methodology of linear parameter varying control synthesis of f-16 aircraft system. *J. Guid. Control. Dyn.* **2001**, *25*, 1040–1048. [\[CrossRef\]](#)
20. Fang, X.; Wu, A.; Shang, Y. Multivariable super twisting based robust trajectory tracking control for small unmanned helicopter. *Math. Probl. Eng.* **2015**, *2021*, 1–13. [\[CrossRef\]](#)
21. Autenrieb, J.; Shin, H.S.; Bacic, M. Development of a neural network-based adaptive nonlinear dynamic inversion controller for a tilt-wing VTOL. *Aircraft* **2019**, *42*, 44–52.
22. Hong, H.T.; Yan, R.; Deng, X.F. Fuzzy sliding mode control of four-rotor aircraft. *J. Jishou Univ.* **2020**, *41*, 31–35.
23. Han, J. From PID to active disturbances rejection control. *IEEE Trans. Ind. Electron.* **2009**, *16*, 900–906. [\[CrossRef\]](#)
24. Ai, S.; Song, J.; Cai, G.; Zhao, K. Active Fault-Tolerant Control for Quadrotor UAV against Sensor Fault Diagnosed by the Auto Sequential Random Forest. *Aerospace* **2022**, *9*, 518. [\[CrossRef\]](#)
25. Zhao, K.; Song, J.; Ai, S.; Xu, X.; Liu, Y. Active Fault-Tolerant Control for Near-Space Hypersonic Vehicles. *Aerospace* **2022**, *9*, 237. [\[CrossRef\]](#)
26. Wang, Z.; Li, J.; Duan, D. Manipulation strategy of tilt quad rotor based on active disturbance rejection control. *Proc. Inst. Mech. Eng. Part G J. Aerosp. Eng.* **2020**, *234*, 1–12. [\[CrossRef\]](#)
27. Wang, Z.; Zhao, H.; Duan, D.; Jiao, Y.; Li, J. Application of improved active disturbance rejection control algorithm in tilt quad rotor. *Chin. J. Aeronaut.* **2020**, *33*, 1625–1641. [\[CrossRef\]](#)

28. Shen, S.; Xu, J. Trajectory tracking active disturbance rejection control of the unmanned helicopter and its parameters tuning. *IEEE Access* **2021**, *9*, 56773–56785. [[CrossRef](#)]
29. Li, Z.B.; Dong, Q.L.; Zhang, X.Y. Impact angle-constrained integrated guidance and control for supersonic skid-to-turn missiles using backstepping with global fast terminal sliding mode control. *Aerosp. Sci. Technol.* **2022**, *122*, 1–17. [[CrossRef](#)]
30. Lungu, M. Backstepping and dynamic inversion control techniques for automatic landing of fixed wing unmanned aerial vehicles. *Aerosp. Sci. Technol.* **2022**, *122*, 1–20. [[CrossRef](#)]
31. Pan, Z.; Chi, C.; Zhang, J. Nonlinear attitude control of tilt-rotor aircraft based on active disturbance rejection sliding mode theory. *Aero Weapon.* **2018**, *58*, 44–49.
32. Welcer, M.; Szczepański, C.; Krawczyk, M. The impact of sensor errors on flight stability. *Aerospace* **2022**, *9*, 169. [[CrossRef](#)]